

## Demonstration of an Alternative Mechanism for G-to-G Cross-Link Formation

Ming Qian and Rainer Glaser\*

Contribution from the Department of Chemistry, University of Missouri-Columbia,  
605 South College Avenue, Columbia, Missouri 65211

Received August 13, 2004; E-mail: glaser@missouri.edu

**Abstract:** The cross-link **dG-to-dG** is an important product of DNA nitrosation. Its formation has commonly been attributed to nucleophilic substitution of  $N_2$  in a guaninediazonium ion by guanine, while recent studies suggest guanine addition to a cyanoamine derivative formed after dediazonation, deprotonation, and pyrimidine ring-opening. The chemical viability of the latter mechanism is supported here by the experimental demonstration of **rG-to-aG** formation via **rG** addition to a synthetic cyanoamine derivative. Thus, all known products of nitrosative guanine deamination are consistent with the postulate of pyrimidine ring-opening. This postulated mechanism not only explains what is already known but also suggests that other products and other cross-links also might be formed in DNA deamination. The study suggests one possible new product: the structure isomer **aG(N1)-to-rG(C2)** of the classical **G(N<sup>2</sup>)-to-G(C2)** cross-link. While the formation of **aG(N<sup>2</sup>)-to-rG(C2)** has been established by chemical synthesis, the structure isomer **aG(N1)-to-rG(C2)** has been assigned tentatively based on its MS/MS spectrum and because this assignment is reasonable from a mechanistic perspective. Density functional calculations show preferences for the amide-iminol tautomer of the classical cross-link **G(N<sup>2</sup>)-to-G(C2)** and the amide-amide tautomer of **G(N1)-to-G(C2)**. Moreover, the results suggest that both cross-links are of comparable thermodynamic stability, and that there are no a priori energetic or structural reasons that would prevent the formation of the structure isomer in the model reaction or in DNA.

### Introduction

DNA oxidizing chemicals are of interest because of their antibiotic, antitumor, carcinogenic, and mutagenic properties.<sup>1,2</sup> An important class of DNA damaging agents includes nitrates, nitrites, and nitrogen oxides because of the dietary and environmental exposure of humans to these substances.<sup>3–5</sup> Toxicological studies of deamination became more significant in the past decade because it was recognized that endogenous nitric oxide<sup>6,7</sup> causes nitrosation<sup>8–11</sup> and that this process is accelerated by chronic inflammatory diseases.<sup>12–14</sup> Several human DNA repair genes have been identified, and some of

these are thought to be involved in cross-link repair.<sup>15,16</sup> Details of the detection of the DNA damage, the signaling to initiate repair, and the actual DNA repair are only now emerging.<sup>17</sup> Deamination chemistry thus contributes to genomic instability directly by causing DNA damage and indirectly by causing damage to any part of the repair mechanisms.

Xanthosine is the main product of guanosine deamination, and the formation of xanthine by deamination of guanine has been known since the very discovery of guanine.<sup>18</sup> The second major product, oxanosine, was discovered only recently by Suzuki et al.<sup>19</sup> and described also by Shuker et al.<sup>20</sup> and Dedon et al.<sup>21</sup> While oxanosine can be formed in yields of up to 20%, its yield varies with conditions, and this might have been one reason for its late discovery in 1996. Our particular interest here lies with the interstrand cross-link **dG-to-dG**, which is a minor product of major significance. As early as 1961, Geiduschek discussed the possibility of interstrand cross-links formed by nitrous acid.<sup>22,23</sup> Initially, there was some discussion that the

- (1) Burrows, C. J.; Muller, J. G. *Chem. Rev.* **1998**, *98*, 1109–1152.
- (2) Marnett, L. J.; Burcham, P. C. *Chem. Res. Toxicol.* **1993**, *6*, 771–785.
- (3) *The Health Effect of Nitrate, Nitrite, and N-Nitroso Compounds*. Committee on Nitrite and Alternative Curing Agents in Food; National Academy Press: Washington, DC, 1981.
- (4) Furia, T. E. *Handbook of Food Additives*, 2nd ed.; CRC Press: Cleveland, OH, 1972; pp 150–155.
- (5) Wakabayashi, K. In *Mutation and the Environment, Part E*; Albertini, R. J., Ed.; Wiley-Liss, Inc.: New York, 1990; pp 107–116.
- (6) Culotta, E.; Koshland, D. E. *Science* **1991**, *258*, 1862–1865.
- (7) Marnett, L. J. *Chem. Res. Toxicol.* **1996**, *9*, 807–808.
- (8) Wink, D. A.; Kasprzak, K. S.; Maragos, C. M.; Elespuru, R. K.; Misra, M.; Dunams, T. M.; Cebula, T. A.; Koch, W. H.; Andrews, A. W.; Allen, J. S.; Keefer, L. K. *Science* **1991**, *254*, 1001–1003.
- (9) Kosaka, H.; Wishnok, J. S.; Miwa, M.; Leaf, C. D.; Tannenbaum, S. R. *Carcinogenesis* **1989**, *10*, 563–566.
- (10) Davis, K. L.; Martin, E.; Turko, I. V.; Murad, F. *Annu. Rev. Pharmacol. Toxicol.* **2001**, *41*, 203–236.
- (11) Jackson, A. L.; Loeb, L. A. *Mutat. Res.* **2001**, *477*, 7–21.
- (12) Ohshima, H.; Bartsch, H. *Mutat. Res.* **1994**, *305*, 253–264.
- (13) deRojas-Walker, T.; Tamir, S.; Ji, H.; Wishnok, J. S.; Tannenbaum, S. R. *Chem. Res. Toxicol.* **1995**, *8*, 473–477.
- (14) Tamir, S.; Tannenbaum, S. R. *Biochim. Biophys. Acta* **1996**, *1288*, F31–F36.

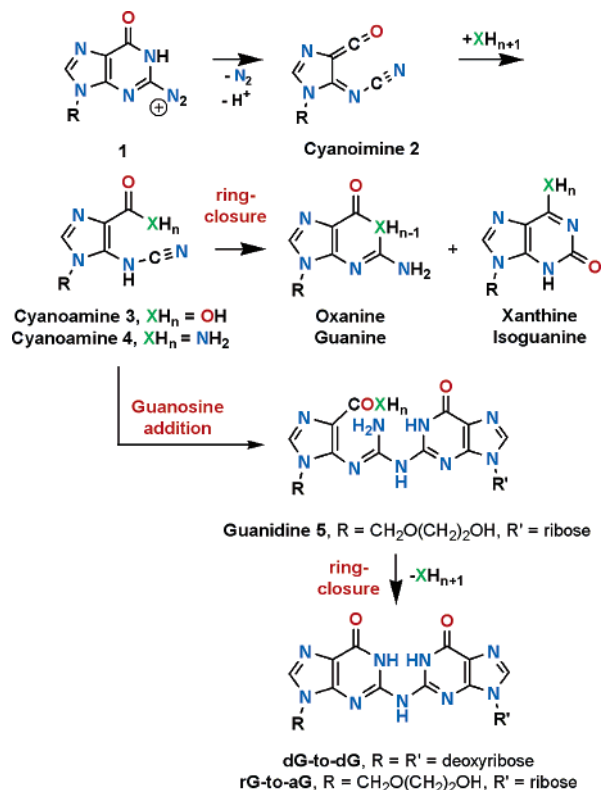
- (15) Wood, R. D.; Mitchell, M.; Sgouros, J.; Lindahl, T. *Science* **2001**, *291*, 1284–1289.
- (16) Schärer, O. D. *Angew. Chem., Int. Ed.* **2003**, *42*, 2946–2974.
- (17) Rouse, J.; Jackson, S. P. *Science* **2002**, *297*, 547–551.
- (18) Strecker, A. *Ann.* **1861**, *118*, 151–177.
- (19) Suzuki, T.; Yamaoka, R.; Nishi, M.; Ide, H.; Makino, K. *J. Am. Chem. Soc.* **1996**, *118*, 2515–2516.
- (20) Lucas, L. T.; Gatehouse, D.; Shuker, E. G. *J. Biol. Chem.* **1999**, *274*, 18319–18326.
- (21) Dong, M.; Wang, C.; Deen, W. M.; Dedon, P. C. *Chem. Res. Toxicol.* **2003**, *16*, 1044–1055.
- (22) Geiduschek, E. P. *Proc. Natl. Acad. Sci. U.S.A.* **1961**, *47*, 950–955.
- (23) Geiduschek, E. P. *J. Mol. Biol.* **1963**, *8*, 377–391.

cross-link formation occurs without depurination<sup>24</sup> and would be a derivative of xanthosine.<sup>25</sup> The cross-link structures became clear in 1977 when Shapiro et al. isolated and partially characterized the cross-links **dG-to-dG** and **dG-to-dA** formed in treatments of calf thymus DNA with nitric acid.<sup>26,27</sup> The **dG-to-dG** cross-link also can be formed by nitric oxide (NO).<sup>28</sup> Hopkins et al. showed in the early 1990s that the **dG-to-dG** interstrand cross-link is formed with sequence specificity in 5'-CG over 5'-GC.<sup>29,30</sup> In the last five years, chemical syntheses of **dG-to-dG** have provided direct confirmation of the cross-link structure.<sup>31–33</sup>

The commonly discussed reaction mechanism for nitrosative guanosine deamination postulates the guanosinediazonium ion **1d** (**1**, R = deoxyribose) as the key intermediate formed by the nitrosation of the exocyclic primary amino group of guanosine. This assumption explains the formation of xanthosine and of the interstrand cross-links **dG-to-dG** and **dG-to-dA**, respectively, by aromatic nucleophilic substitutions of N<sub>2</sub> by water or by the amino group of a guanosine or an adenosine of the opposite stand, respectively. Recent theoretical studies revealed that guaninediazonium ion **1** (R = H) is much less stable than had been thought, and that pyrimidine ring-opening occurs with dediazonation and deprotonation to form cyanoimines **2**.<sup>34–36</sup> Oxanosine formation requires such a pyrimidine ring-opening, and recent labeling studies established the intermediacy of 5-cyanoimino-4-oxomethylene-4,5-dihydroimidazole and 5-cyanoamino-4-imidazolecarboxylic acid in nitrosative guanosine deamination.<sup>37</sup> On the other hand, the formations of xanthosine and of the cross-links may proceed with or without pyrimidine ring-opening or by a combination of these paths, and which of these options is realized might depend on the environment (solution, DNA, and pH). We postulate with the principle of parsimony<sup>38</sup> that all products are formed from the same common intermediate, the cyanoimine **2**, and it has been our goal to explore whether this option is chemically viable.

We are exploring the chemistry of the cyanoamines **4**. The CH<sub>2</sub>OCH<sub>2</sub>OH group is a simple glycoside mimic, and compounds with this R group are designated by **a** (derivative of acyclovir). Cyanoamines **3** and **4** are the products of the 1,4-addition of H-XH<sub>n</sub> to cyanoimine **2**, and this addition is very fast because of the zwitterionic nature of cyanoimine **2**.<sup>39,40</sup> The 5-cyanoamino-4-imidazolecarboxamide **4a** was targeted because of practical advantages in the preparation of the cyanoamino

**Scheme 1.** Experimental Demonstration of Cross-Link **rG-to-aG** Formation by Reaction of **4a** (R = CH<sub>2</sub>OCH<sub>2</sub>OH) with Guanosine **rG**



function in the presence of a carboxamide and for a conceptual reason (vide infra). We described the synthesis of **4a** and demonstrated its recyclization to guanosine **aG** and isoguanosine **aIG** in analogy to the formations of xanthosine and oxanosine from **3**, respectively.<sup>41</sup> Here, we report experiments that demonstrate the formation of the cross-link **rG-to-aG** by addition of guanosine **rG** (R' = ribose) to cyanoamine **4a**.<sup>42</sup>

## Results and Discussion

**Strategy: Giving the Bimolecular Reaction a Chance in the Absence of Templating.** The most direct evidence for the formation of **dG-to-dG** by guanosine addition to a cyanoamine **4** would involve the synthesis of oligonucleotides with **4d** in place of **dG** and the detection of **dG-to-dG** cross-link formation. This experiment is impossible because **4d** cannot be generated in an oligonucleotide via a targeted synthesis. The next best strategy involves the synthesis of a cyanoamine **4** and the study of its bimolecular guanosine addition. This strategy could be improved by tethering the guanosine to the cyanoamine, and we were contemplating such approaches for some time before we gathered enough courage to even try the untethered reaction, which to our surprise, worked quite well!

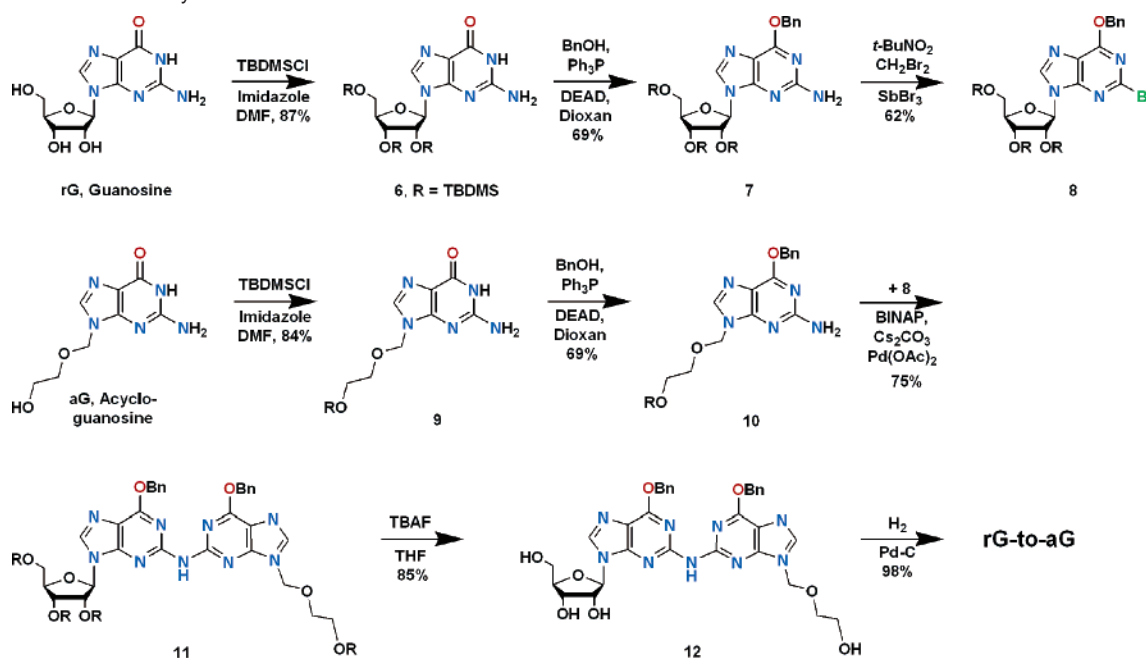
The recyclizations of cyanoamine **4a** to isoguanosine **aIG** and guanosine **aG** are very fast.<sup>41</sup> The only chance to observe any intermolecular reaction in solution requires high concentrations of the starting materials (of **rG** in particular) to increase the rate of the bimolecular addition. Due to the poor solubility of guanosine **rG** in water, we therefore studied the reaction in

- (24) Verly, W. G.; Lacroix, M. *Biochim. Biophys. Acta* **1975**, *414*, 185–192.  
 (25) Burnotte, J.; Verly, W. H. *J. Biol. Chem.* **1971**, *246*, 5914–5918.  
 (26) Shapiro, R.; Dubelman, S.; Feinberg, A. M.; Crain, P. F.; McCloskey, A. M. *J. Am. Chem. Soc.* **1977**, *99*, 302–303.  
 (27) Dubelman, S.; Shapiro, R. *Nucleic Acids Res.* **1977**, *4*, 1815–1827.  
 (28) Caulfield, J. L.; Wishnok, J. S.; Tannenbaum, S. R. *Chem. Res. Toxicol.* **2003**, *16*, 571–574.  
 (29) Kirchner, J. J.; Hopkins, P. B. *J. Am. Chem. Soc.* **1991**, *113*, 4681–4682.  
 (30) Kirchner, J. J.; Sigurdsson, S. T.; Hopkins, P. B. *J. Am. Chem. Soc.* **1992**, *114*, 4021–4027.  
 (31) Harwood, E. A.; Sigurdsson, S. T.; Edfeldt, N. B. F.; Reid, B. R.; Hopkins, P. B. *J. Am. Chem. Soc.* **1999**, *121*, 5081–5082.  
 (32) Harwood, E. A.; Hopkins, P. B.; Sigurdsson, S. T. *J. Org. Chem.* **2000**, *65*, 2959–2964.  
 (33) De Riccardis, F.; Johnson, F. *Org. Lett.* **2000**, *2*, 293–295.  
 (34) Glaser, R.; Son, M. S. *J. Am. Chem. Soc.* **1996**, *118*, 10942–10943.  
 (35) Glaser, R.; Rayat, S.; Lewis, M.; Son, M.-S.; Meyer, S. *J. Am. Chem. Soc.* **1999**, *121*, 6108–6119.  
 (36) Glaser, R.; Lewis, M. *Org. Lett.* **1999**, *1*, 273–276.  
 (37) Rayat, S.; Majumdar, P.; Tipton, P.; Glaser, R. *J. Am. Chem. Soc.* **2004**, *126*, 9960–9969.  
 (38) Wassermann, G. D. *From Occam's Razor to the Roots of Consciousness: 20 Essays on Philosophy, Philosophy of Science and Philosophy of Mind*; Avebury: Aldershot, U.K., 1997.  
 (39) Rayat, S.; Glaser, R. *J. Org. Chem.* **2003**, *68*, 9882–9892.  
 (40) Rayat, S.; Wu, Z.; Glaser, R. *Chem. Res. Toxicol.* **2004**, *17*, 1157–1169.

(41) Qian, M.; Glaser, R. *J. Am. Chem. Soc.* **2004**, *126*, 2274–2275.

(42) **rG** was used for economical reasons, and no significant differences would be expected for **dG**.

Scheme 2. Outline of the Synthesis of rG-to-aG



DMSO. All prior reports of cross-link formation of natural or synthetic DNA and oligonucleotides with  $\text{HNO}_2$  or NO in aqueous buffer solution were carried out with low DNA concentrations because minimal structural distortions of the duplex shape suffice to position the amino N atom of the nucleophile **dG** in the proximity of the reactive intermediate generated by **dG** deamination on the opposite strand. These proximity effects are important and were cited to explain the sequence specificity.<sup>29,30</sup> Cross-link formation caused by nitrous acid is preferred at 5'-CG positions compared to 5'-GC positions because the B conformation of 5'-CG positions the amino group of the nucleophile **dG** well, while a 3 Å base pair sliding is required to achieve proximity in 5'-GC. But even with all the advantages provided by the DNA environment, cross-link formation in DNA still hardly can compete with hydrolyses to form xanthine and oxanine products (1 in 4 deamination events). The yield of **dG-to-dG** was ca. 0.06% in Shapiro's  $\text{HNO}_2$  treatment of calf thymus DNA,<sup>26</sup> and the Hopkins group reported a cross-link yield of 2.4% in their synthetic oligodeoxynucleotide with the 5'-CG sequence.<sup>29,30</sup> Bimolecular reactions also are accelerated by increases in temperature because the collision frequency increases, and we obtained detectable amount of products of the bimolecular reaction at about 80 °C. In DNA work, of course, no such temperature increases are needed because proximity is established by the environment. Finally, we employed different R groups on the cyanoamine **4a** and the guanosine **rG** to ensure that any detected cross-link was indeed the product of bimolecular addition rather than some sort of dimerization.

**Synthesis of rG-to-aG Cross-Link.** The reliable detection of tiny amounts of cross-link in large amounts of products of unimolecular cyclization poses an analytical challenge. We synthesized and fully characterized **rG-to-aG** and thereby made possible the tuning of the mass spectrometer to optimal sensitivity for **rG-to-aG**. The synthesis of the cross-link **rG-to-aG** is outlined in Scheme 2 and employs chemistry developed by the group of Hopkins<sup>31,32</sup> and by De Riccardis and Johnson.<sup>33</sup> The protections of the 2'-, 3'-, and 5'-OH groups in ribose of

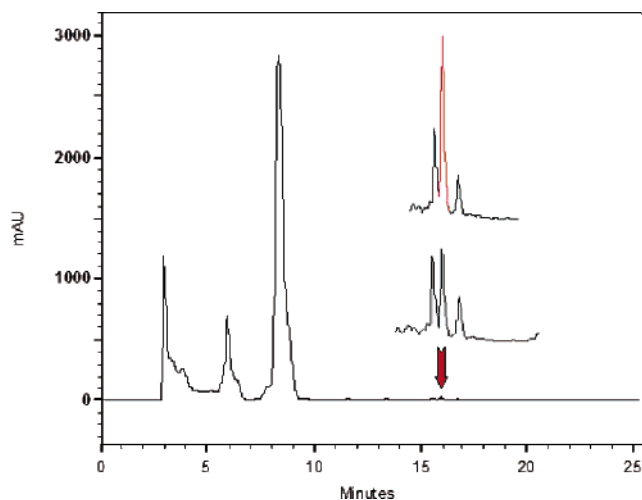
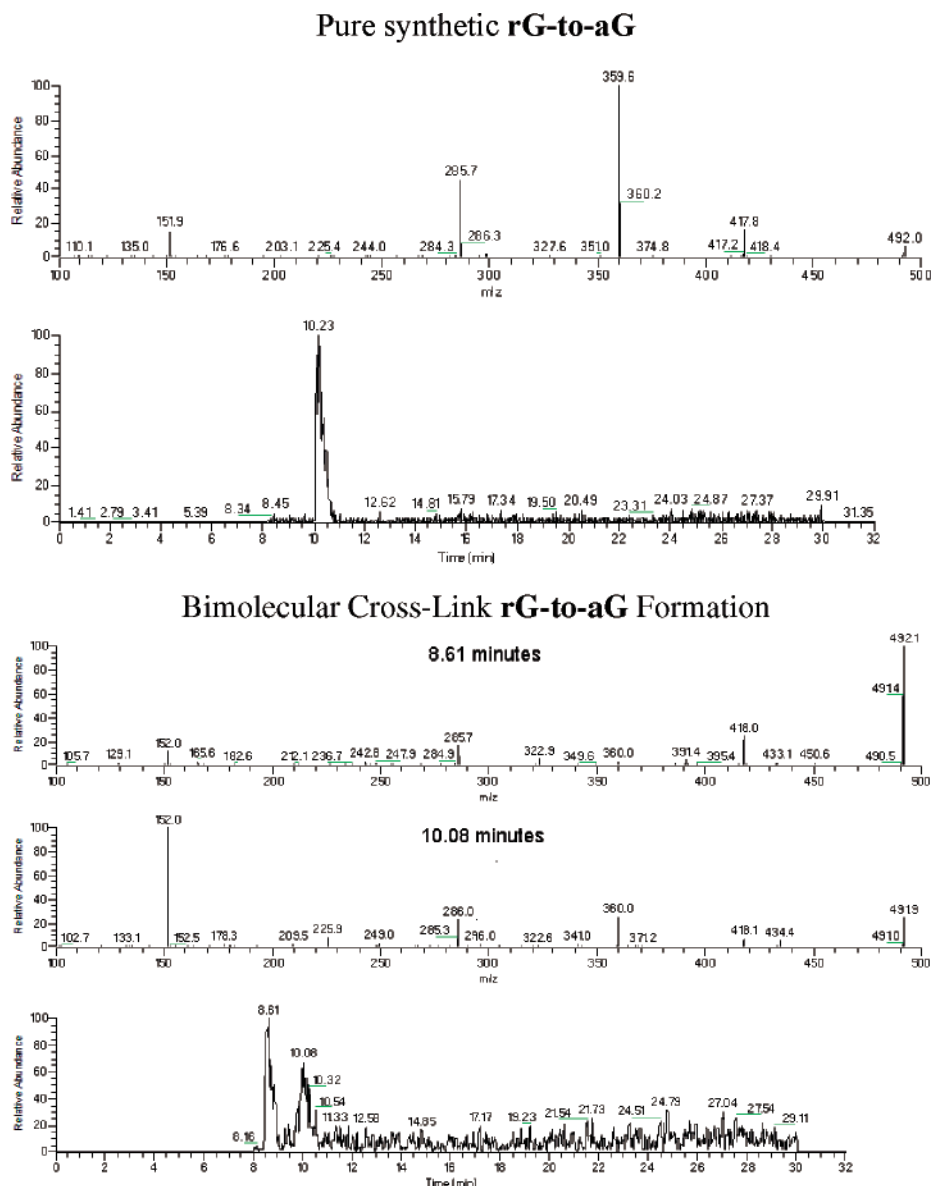


Figure 1. HPLC chromatogram of the product of the reaction between cyanoamine **4a** and guanosine **rG** demonstrates **rG-to-aG** formation. The cross-link was identified by the addition of synthetic and authenticated cross-link **rG-to-aG** (increased peak, in red, with retention time of 16.0 min).

**rG** and of the OH group of **aG** were carried out by reaction of *tert*-butyldimethylsilyl chloride (TBDMSCl) in the presence of imidazole in DMF solution. The O6 atoms of **6** and **9** were subsequently protected by conversion into the benzyl ethers **7** and **10**, respectively. Then, **7** was brominated by diazotization with *tert*-butylnitrite in methylene bromide and treatment with  $\text{SbBr}_3$  to afford **8**. The coupling reaction of **8** to **10** was catalyzed by 10 mol % palladium acetate, 15 mol % ( $\pm$ )-BINAP, and the presence of  $\text{Cs}_2\text{CO}_3$  and gave **11** in 75% yield. The silyl protecting groups were removed with tetrabutylammonium fluoride (TBAF), and the benzyl protecting groups were removed by hydrogenation. The product **rG-to-aG** was fully characterized by  $^1\text{H}$  and  $^{13}\text{C}$  NMR spectroscopy and mass spectrometry. Ours is the first unsymmetrical ( $R \neq R'$ ) **G-to-G** cross-link, and the  $^1\text{H}$  NMR spectrum of **rG-to-aG** shows two aromatic nonexchangeable hydrogens (C8 positions).

**Cross-Link Formation via Cyanoamine.** The cross-link **rG-**



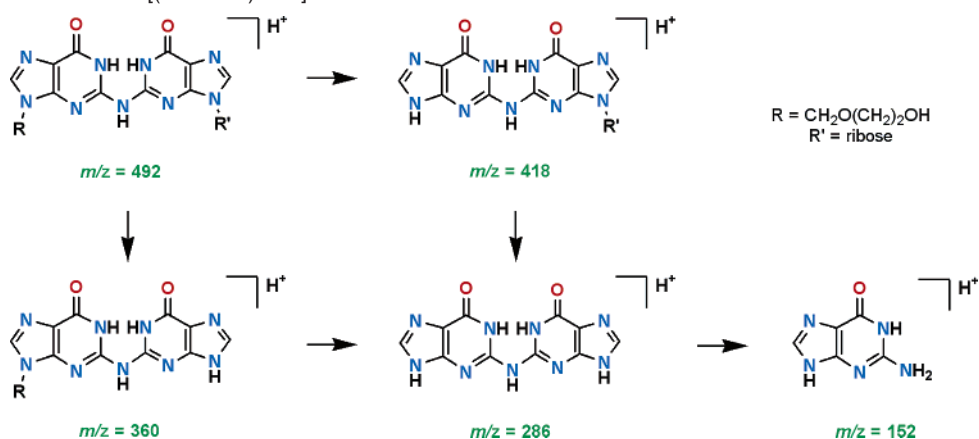
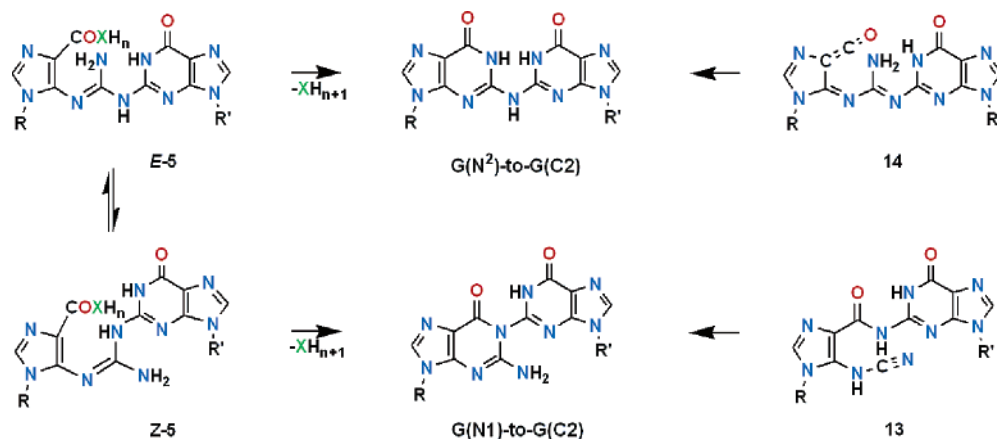
**Figure 2.** LC–MS/MS spectra of pure synthetic **rG-to-aG** and cross-links formed by the bimolecular reaction of cyanoamine **4a** and guanosine **rG**. In the top graph is shown the MS/MS spectrum of the parent ion  $[(\mathbf{rG-to-aG}) + \mathbf{H}]^+$  at  $m/z = 492$  of the pure synthetic cross-link, with a retention time in the mass trace of about 10 min (mass trace shown below). For the bimolecular cross-link formation, two MS/MS spectra are shown for two parent ions with that same mass  $m/z = 492$ , but retention times of about 8 and 10 min.

**to-aG** was formed by **rG** addition to cyanoamine **4a** in DMSO solution at 80 °C in the course of 120 min. The HPLC chromatogram of the reaction mixture is shown in Figure 1. The three large peaks correspond to unreacted cyanoamine **4a**, the products of intramolecular cyclization [isoguanine **aIG** and guanine **aG** (overlapping)], and unreacted guanosine **rG**. The inset shows three minor peaks, and the intensity of the central one increased upon addition of synthetic **rG-to-aG**. Hence, **rG-to-aG** was formed in the bimolecular reaction.

The LC–MS/MS of the  $[(\mathbf{rG-to-aG}) + \mathbf{H}]^+$  parent ion,  $m/z = 492$ , of synthetic **rG-to-aG** is shown in the top graphs of Figure 2. The concentration of this solution was 0.02 mM, so that the intensity of the **rG-to-aG** peak in the LC chromatogram was about the same as that for the corresponding peak in the bimolecular reaction mixture. The fragmentation pattern is described in Scheme 3. The  $m/z = 286$  typically occurs in MS/MS spectra of **dG-to-dG** obtained by treating DNA with  $\text{HNO}_2$  and subsequent digestion.<sup>26,29</sup>

The LC–MS/MS analysis of the bimolecular cross-link formation shows that *two structure isomeric cross-links are formed*; there are two parent ions with  $m/z = 492$  from products with different retention times. The MS/MS analysis of the parent ions with  $m/z = 492$  shows that only the central one of the three minor peaks in the HPLC chromatogram of Figure 1 causes a significant ion concentration. The cross-link isomer detected in the mass trace at a retention time of about 8 min had escaped UV detection at 254 nm in LC chromatograms (e.g., Figure 1). In Figure 8 of the Supporting Information, we provide UV and mass traces, which show that the peak at 8 min does not correspond to any of the peaks around 16 min in Figure 1.

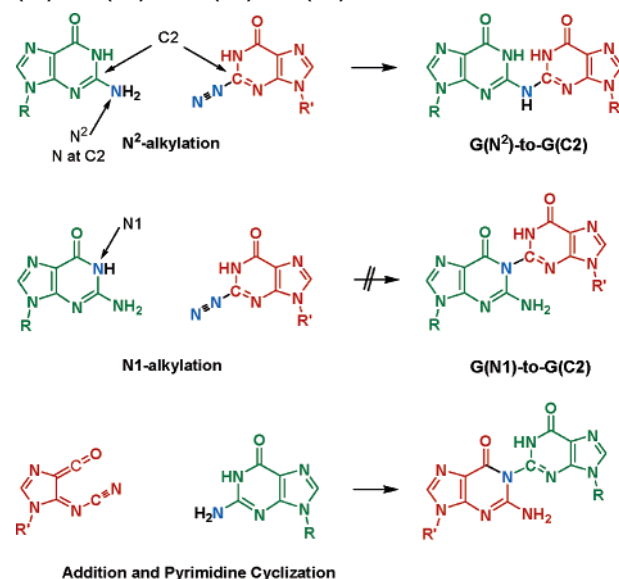
The MS/MS spectrum of the reaction product with the retention time of about 10 min (below center, Figure 2) has essentially the same retention time as that of synthetic **rG-to-aG**, and its fragmentation pattern is identical to the MS/MS spectrum of pure synthetic **rG-to-aG** (top, Figure 2). There are intensity differences in the MS/MS spectra of the pure cross-

**Scheme 3.** Fragmentation of the [(rG-to-aG) + H]<sup>+</sup> Parent Ion with *m/z* = 492**Scheme 4.** Formations of Cross-Links **G(N<sup>2</sup>)-to-G(C2)** and **G(N1)-to-G(C2)**

link and the cross-link in the reaction mixture (Figure 2), and the cause of these intensity differences is not clear. We have recorded the MS/MS spectrum of the reaction mixture containing the cross-links formed by the bimolecular reaction of **4a** and **rG** after addition of some pure synthetic **rG-to-aG**, and this spectrum (Figure 8 in the Supporting Information) demonstrates beyond any doubt that the classical cross-link is formed. We also recorded LC-MS/MS spectra in selective reaction monitoring (SRM) mode, monitoring the parent ion *m/z* = 492 and the product ion *m/z* = 360 to further corroborate the identity of the synthetic **rG-to-aG** and the cross-link made by the addition chemistry.

The other MS/MS spectrum corresponds to the peak with a mass trace retention time of about 8 min. The proposed structure of the second cross-link is shown in Scheme 4 along with a proposal for its formation. Both amino N atoms of guanidine **5** can attack the carboxamido group, leading to either the classical or the new **rG-to-aG** cross-link, depending on whether the guanidine is in the (*E*)- or (*Z*)-configuration about the C=N double bond, respectively. When this possibility for structure isomerism of the cross-links is recognized, it becomes immediately obvious that their fragmentation patterns are alike as well because they lead to structure isomeric ions.

There is a need to differentiate clearly between these structure isomers, and we suggest the following formalism. Both cross-links formally link a guanine fragment deaminated at C2 to either the N<sup>2</sup> or the N1 atom of a complete guanine. Hence, we refer to the classical cross-link as **G(N<sup>2</sup>)-to-G(C2)** and to its isomer as **G(N1)-to-G(C2)**. This is a *formal* nomenclature

**Scheme 5.** Positions of the "Intact Guanine" (green) and of the "Deaminated Guanine" (red) in the **G-to-G** Cross-Links, **G(N<sup>2</sup>)-to-G(C2)** and **G(N1)-to-G(C2)**

indeed as it is clear that **G(N1)-to-G(C2)** is not formed by alkylation at N1! This important point is illustrated in Scheme 5, where color is used to differentiate between the guanines that enter the cross-link either intact or deaminated. The formal N1 alkylation and the actual mechanisms involving addition and cyclization result in **G(N1)-to-G(C2)** cross-links in which the deaminated guanine occupy different positions. In other words,

**Table 1.** Total and Relative Energies of **G-to-G** Cross-Link Structures

structure isomer, tautomer	Relative Energy (kcal/mol)		
	B3LYP/6-31G*	B3LYP/6-31+G**/ B3LYP/6-31G*	IPCM, DMSO B3LYP/6-31+G**/ B3LYP/6-31G*
<b>G(N<sup>2</sup>)-to-G(C2)</b> , amide–amide	0.22	1.47	0.12
<b>G(N1)-to-G(C2)</b> , amide–amide	8.77	10.95	-8.72
<b>G(N<sup>2</sup>)-to-G(C2)</b> , amide–iminol	0.00	0.00	0.00
<b>G(N1)-to-G(C2)</b> , amide–iminol	14.58	14.03	11.56

the positions of R and R' differ in **G(N1)-to-G(C2)**, depending on the mechanism of the cross-link's formation. While there is only one **G(N<sup>2</sup>)-to-G(C2)** cross-link, **rG(N<sup>2</sup>)-to-aG(C2)** is the same as **aG(N<sup>2</sup>)-to-rG(C2)**; the cross-links **rG(N1)-to-aG(C2)** and **aG(N1)-to-rG(C2)** are isomers, and only **aG(N1)-to-rG(C2)** is formed.

**Two Reaction Pathways to G(N1)-to-G(C2).** At the beginning, we stated that we are interested in the cyanoamines **3** (X = OH) and **4** (X = NH<sub>2</sub>). Cyanoamines **3** are water adducts of the cyanoimines **2**, and cyanoamines **4** are their amine adducts. We are studying **4** for practical reasons (vide supra) and for an important conceptual reason which is now becoming clear: cyanoamine **4** is the simplest model of the DNA base adduct **13!** Since **4a** cyclizes to guanosine<sup>41</sup> and because of the **G(N1)-to-G(C2)** formation shown here, we have established that there are two possible reaction channels leading to **G(N1)-to-G(C2)** in DNA. Similar logic would suggest that **14**, formed by addition of guanine to the cyanoimine function of **2**, might provide a path to the classical cross-link **G(N<sup>2</sup>)-to-G(C2)**. However, the electronic structure of cyanoimines suggests that nucleophilic addition to the ketene moiety is faster<sup>39</sup> and it also leads to aromatization. Any classical cross-link **G(N<sup>2</sup>)-to-G(C2)** formed via pyrimidine ring-opening most likely passed through a guanidine (*E*)-5.

**Structures of G-to-G Cross-Links.** Density functional theory at the B3LYP/6-31G\* level<sup>43</sup> was employed to determine the structures of the **G-to-G** cross-links. The amide–amide and amide–iminol tautomers were considered for both structure isomers. Relative energies are given in Table 1, and the structures are shown in Figure 3.

The commonly drawn amide–amide tautomer of **G(N<sup>2</sup>)-to-G(C2)** greatly suffers from carbonyl dipole alignment and (N1, N1') lone pair repulsion, and rotation about the C2–N bond leads to the conformation with an N1–H···N3 hydrogen bond (197.0 pm). While this rotation is possible for the free molecule, it is not possible in DNA, and **G(N<sup>2</sup>)-to-G(C2)** should greatly prefer the amide–iminol tautomer in DNA. This tautomer features an N1–H···N1 hydrogen bond (198.8 pm) and a distance of 975.1 pm between the R groups at N9. The amide–amide tautomer of structure isomer **G(N1)-to-G(C2)** features two hydrogen bonds, N–H···N3 (194.5 pm) and N1–H···O6 (191.5 pm), some propeller distortion, and a distance of 917.3 pm between the R groups at N9, and this tautomer is only 8.8 kcal/mol less stable than the amide–iminol tautomer of the

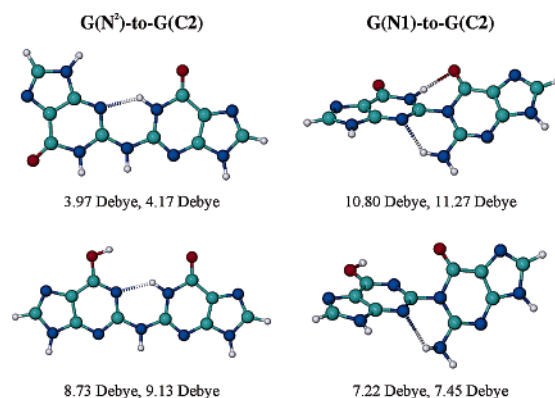


**Figure 3.** Molecular models of the B3LYP/6-31G\* structures are shown of the classical cross-link **G(N<sup>2</sup>)-to-G(C2)**, amide–amide (top) and amide–iminol (bottom) tautomers, and of the structure isomer, **G(N1)-to-G(C2)**, again amide–amide (top) and amide–iminol (bottom) tautomers. Dipole moments computed at B3LYP/6-31G\* and B3LYP/6-31+G\*\*/B3LYP/6-31G\* levels are given in that order.

classical structure. The amide–iminol tautomer is clearly disadvantaged; while the N–H···N3 hydrogen bond (219.2 pm) is maintained, the distance between the carbonyl–O and the hydroxyl group is too long (430.1 pm) for a second hydrogen bond.

Structures are usually well reproduced at the B3LYP/6-31G\* level. Relative energies, on the other hand, are more dependent on the theoretical level, and they also are solvent dependent. Hence, we also computed relative energies with the fully polarized and diffuse function augmented 6-31+G\*\* basis set for the isolated structures, B3LYP/6-31+G\*\*/B3LYP/6-31G\*, and with implicit solvation<sup>44</sup> effects included via the isodensity polarizable continuum model,<sup>45</sup> IPCM (B3LYP/6-31+G\*\*/B3LYP/6-31G\*). In particular, these additional basis functions allow for improved descriptions of the hydrogen bonds because the sets of diffuse s- and p-functions improve the hydrogen bond donor atoms O and N, and the sets of p-polarization function should be beneficial for the H-atoms involved in hydrogen bonding. The data in Table 1 show only modest changes of the relative energies in the gas phase (up to 2 kcal/mol), while a remarkable solvent effect is found on the relative stability of the amide–amide tautomer of **G(N1)-to-G(C2)**. These dipole moments of the cross-links vary significantly (Figure 3), and the stabilization by solvent roughly parallels molecular polarity. Yet, the solvation effect on the amide–amide tautomer of **G(N1)-to-G(C2)** is remarkable even in light of the fact that this structure has the largest dipole moment among all the isomers. The number of hydrogen bond donors and hydrogen bond acceptors available for any specific solvation also differs in the isomers, and in particular, the amide–amide tautomer of **G(N1)-to-G(C2)** has the least number of available hydrogen bond donors.

The major conclusions from the theoretical study are as follows. (1) The amide–amide and the amide–iminol tautomers of the classical **G-to-G** cross-link are almost isoenergetic. (2) In DNA, the amide–iminol tautomers of the classical **G-to-G** cross-link are greatly favored because the accommodation of the amide–amide tautomer would require a 180° rotation about

(44) Cramer, C. J.; Truhlar, D. G. *Chem. Rev.* **1999**, *99*, 2161.

(45) Foresman, J. B.; Keith, T. A.; Wiberg, K. B.; Snoonian, J.; Frisch, M. J. *J. Phys. Chem.* **1996**, *100*, 16098. (b) Pomelli, C. S.; Tomasi, J. *J. Phys. Chem. A* **1997**, *101*, 3561.

(43) Cramer, C. J. *Computational Chemistry*; John Wiley & Sons: New York, 2001.

the C2–NH bond, and as discussed above, that would cause disruption of hydrogen bonding and dipole–dipole repulsion. Apparently, this tautomer has never been discussed in the more than 40 year history of the cross-link, and there is every reason to expect this amide–iminol tautomer to occur in DNA. (3) The relative stabilities of the **G-to-G** structure isomers show that there is no thermodynamic reason for the preferred formation of the classical cross-link, and the product formation must be under kinetic control. (4) The distances between the N9 and N9' atoms in the structures of the structure isomeric cross-links are such that the formation of either cross-link would not be impeded by constraints on the distances between the sugars in ds-DNA. For the cross-link formation to occur in DNA, many additional conditions need to be met.

## Conclusion

We have demonstrated the chemical viability of **rG-to-aG** formation via **rG** addition to a synthetic cyanoamine derivative **4a**. Hence, we have established an alternative to the common hypothesis that assumes **G-to-G** cross-link formation to occur by direct nucleophilic aromatic substitution of a guaninediazonium ion by a guanosine. This alternative hypothesis has the attractive feature that all known products of nitrosative guanine deamination can be consistently explained with the postulate of pyrimidine ring-opening. This postulated mechanism not only explains what is already known but also suggests that other products and other cross-links also might be formed in DNA deamination.

Our study suggests one possible “other product”: the structure isomer **G(N1)-to-G(C2)** of the classical **G(N2)-to-G(C2)** cross-link. While the formation of **aG(N2)-to-rG(C2)** has been established by chemical synthesis, the structure isomer **aG(N1)-to-rG(C2)** has been assigned based on its MS/MS spectrum because this assignment is reasonable from a mechanistic perspective and because the computational study does not suggest any reason that would prevent its formation. Both cross-links are structurally possible in DNA with similar distances between the N9 sugars. Since **G(N1)-to-G(C2)** has not been detected to date, this cross-link apparently is formed in low yield in DNA deamination, if it is formed at all. Prior to the present study, there was no reason to expect the formation of the structure isomer and there has not been any such discussion. Because of the results of the present study, there now is a compelling reason to synthesize the new **G-to-G** cross-link, both to confirm the tentative assignment and to begin the search for this cross-link in DNA deamination. This case exemplifies well the significant role of studies of reaction mechanisms to guide searches for new kinds of chemical DNA damage, and this role is particularly important when very small amounts of damage are to be detected.

## Experimental Section

**General Methods.** <sup>13</sup>C and <sup>1</sup>H NMR spectra were collected on DRX 500 and ARX 250 MHz spectrometers, using *d*<sub>6</sub>-DMSO and CD<sub>3</sub>Cl as solvents. High-resolution MS studies were performed by the Mass Spectrometry Laboratory of the Department of Chemistry, The Ohio State University.

**Materials.** 1-[(2-Hydroxyethoxy)methyl]-5-cyanoamine-4-imidazolecarboxamide **4a** was prepared as described previously by us elsewhere.<sup>41</sup> Other starting materials and solvents were commercially available and were used without further purification.

**HPLC Analysis.** The HPLC analysis was carried out with a Shimadzu system equipped with an SPD-M10Avp photodiode array detector. For system 1, we used Waters XTerra Prep MS C18, 10 μm 10 × 250 mm column, monitoring at 254 nm, and elution at a flow rate of 6.0 mL/min with a gradient from 3% CH<sub>3</sub>CN in 10 mM ammonium acetate (pH 7) to 30% CH<sub>3</sub>CN for the first 17 min, followed by an increase to 60% CH<sub>3</sub>CN over 5 min, then an increase to 70% CH<sub>3</sub>CN in the next 5 min, then reversed to 3% CH<sub>3</sub>CN over 5 min, and finally eluting at 3% CH<sub>3</sub>CN over the last 2 min. This system was used for collecting the synthetic cross-link **rG-to-aG**. For system 2, we used the same column, flow rate, and detection as with system 1, but an elution gradient from 1 to 60% aqueous CH<sub>3</sub>CN over the course of 30 min. System 2 was used for desalting. For system 3, we employed Waters XTerra C18, 5 μm, 4.5 × 250 mm analytical column, and flow rate of 1 mL/min, with the same gradient as that used in system 1. System 3 was used for the analysis of the mixture of the cross-link-forming reaction and the LC–MS analysis.

**Mass Spectrometric Analysis.** LC–MS studies were performed with a Thermo Finnigan TSQ7000 mass spectrometer, equipped with an electrospray ionization (ESI) source and operated in the positive ion mode, LC system with P4000 pump, AS3000 auto sampler, and UV6000 photodiode array detector. To tune the mass spectrometer, the solution of the synthetic **rG-to-aG** (0.02 mM, flowing at a rate of 20 μL/min) was continuously mixed with a solution of 27% aqueous CH<sub>3</sub>CN (flowing at a rate of 1 mL/min), and the mixture was infused into the electrospray source to determine the optimum instrument settings. The LC–MS and LC–MS/MS analyses were carried out with analytical system 3 (vide supra) using both full scan and selective reaction monitoring (SRM) detection modes.

**5'-O,3'-O,2'-O-Tris(tert-butylidimethylsilyl)-6-O-benzylguanosine, 7.** Triphenylphosphine (3.315 g, 12.64 mmol) and 5'-O,3'-O,2'-O-tris(tert-butylidimethylsilyl)guanosine (3.956 g, 12.64 mmol) were placed in a dried flask under vacuum for 15 min. After the flask was refilled with argon, dry dioxane (109 mL) and benzyl alcohol (1.294 g, 12.64 mmol) were added via syringe. Diethylazodicarboxylate (DEAD, 5.8 mL, 12.64 mmol) was added to the resulting suspension slowly via syringe. After the solution became homogeneous, the reaction mixture was stirred for an additional 2 h. Removal of the solvent in vacuo generated a yellow oil, which was redissolved in diethyl ether (37 mL) and left to stand at –20 °C for 1 h. The precipitated white solid was removed by filtration and washed with cold ether. The filtrate was concentrated in vacuo, and the residue was purified by flash chromatography on silica gel (6% ethyl acetate/hexane) to yield 2.89 g of pure **7** (64%) as a white solid. <sup>1</sup>H NMR (250 MHz, *d*<sub>6</sub>-DMSO): δ 8.06 (s, 1H), 7.50–7.36 (m, 5H), 6.47 (s, 2H), 5.83 (d, *J* = 6.9 Hz, 1H), 5.48 (s, 2H), 4.69 (dd, *J* = 6.9, 4.6 Hz, 1H), 4.20 (d, *J* = 3.65 Hz, 1H), 3.95–3.84 (m, 2H), 3.70 (dd, *J* = 11.0, 3.7 Hz, 1H), 0.91 (s, 9H), 0.89 (s, 9H), 0.71 (s, 9H), 0.10 (d, *J* = 4.6 Hz, 6H), 0.08 (d, *J* = 0.8 Hz, 6H), –0.10 (s, 3H), –0.31 (s, 3H). <sup>13</sup>C NMR (500 MHz, *d*<sub>6</sub>-DMSO): δ 160.0, 159.8, 154.6, 137.5, 136.5, 128.5, 128.4, 128.1, 113.7, 85.53, 85.48, 74.7, 72.7, 66.9, 62.8, 25.8, 25.7, 25.5, 18.0, 17.8, 17.5, –4.7, –4.78, –4.8, –5.4, –5.5. ESI–HRMS: *m/e* 738.38386 (M + Na<sup>+</sup>) (calcd 738.387269).

**5'-O,3'-O,2'-O-Tris(tert-butylidimethylsilyl)-6-O-benzyl-2-bromoguanosine, 8.** Amine **7** (583 mg, 0.814 mmol) was dried by dissolving it in anhydrous toluene (6.5 mL) and by removing the solvent in vacuo. To the flask containing the dried amine **rG** was added antimony(III) bromide (413 mg, 1.143 mmol), and the flask was then purged with argon. Anhydrous methylene bromide (9.55 mL), cooled to 0 °C, was added to the reaction flask which was cooled to 0 °C, as well. After the mixture was further cooled to –10 °C, *tert*-butylnitrite (376 μL, 2.85 mmol) was added slowly via syringe. After completion of the nitrite addition, the reaction mixture was stirred for 1 h at –10 °C and then poured into 32.5 mL of a mixture of crushed ice, water, and 1.32 g of sodium bicarbonate. The reaction product was filtered, and the filtrate was extracted with methylene chloride. The combined

organic extracts were dried over sodium sulfate. After filtration, the solvent was removed in vacuo, and a yellow oil was obtained. Flash chromatography with 3% ethyl acetate/hexane as the eluent afforded 392 mg of **8** as a white solid (61.7%). <sup>1</sup>H NMR (500 MHz, *d*<sub>6</sub>-DMSO): δ 8.59 (s, 1H), 7.52 (d, *J* = 6.5 Hz, 2H), 7.43–7.33 (m, 3H), 5.92 (d, *J* = 5.5 Hz, 1H), 5.59 (d, *J* = 2.5 Hz, 2H), 4.88 (t, *J* = 5.0 Hz, 1H), 4.37 (t, *J* = 3.5 Hz, 1H), 4.01–4.00 (m, 2H), 3.73 (dd, *J* = 10.5, 7.5 Hz, 1H), 0.91 (s, 9H), 0.86 (s, 9H), 0.74 (s, 9H), 0.13 (s, 3H), 0.10 (s, 3H), 0.06 (d, *J* = 3.0 Hz, 6H), –0.08 (s, 3H), –0.29 (s, 3H). <sup>13</sup>C NMR (500 MHz, *d*<sub>6</sub>-DMSO): δ 159.8, 152.7, 143.2, 142.1, 135.4, 128.8, 128.5, 120.9, 88.1, 85.0, 73.9, 71.6, 69.1, 61.9, 25.74, 25.68, 25.4, 18.0, 17.7, 17.5, –4.6, –4.9, –5.4, –5.5, –5.6. ESI–HRMS: *m/e* 801.28435 (M + Na<sup>+</sup>) (calcd 801.286881).

**2'-O-(tert-Butyldimethylethylsilyl)acycloguanosine, 9.** Acycloguanosine (200 mg, 0.889 mmol) was added to a mixture of TBDMSCl (294.8 mg, 1.956 mmol) and imidazole (266.19 mg, 3.91 mmol) in 4.5 mL of DMF. The resulting solution was stirred at room temperature overnight. The solvent was removed, and the residue was purified by flash chromatography with 7–10% MeOH/CH<sub>2</sub>Cl<sub>2</sub> as eluent to give 332.4 mg of white product. Recrystallization from MeOH/H<sub>2</sub>O gave 263 mg of analytically pure product **9** in 87% yield. <sup>1</sup>H NMR (500 MHz, *d*<sub>6</sub>-DMSO): δ 10.6 (s, 1H), 7.8 (s, 1H), 6.46 (s, 2H), 5.3 (s, 2H), 3.6 (t, *J* = 4.5 Hz, 2H), 3.5 (t, *J* = 5.0 Hz, 2H), 0.81 (s, 9H), –0.023 (s, 6H). <sup>13</sup>C NMR (500 MHz, *d*<sub>6</sub>-DMSO): δ 156.8, 153.8, 151.4, 137.6, 116.5, 72.1, 70.1, 61.8, 25.7, 17.9, –5.3. ESI–HRMS: *m/e* 362.16214 (M + Na<sup>+</sup>) (calcd 362.161885).

**2'-O-tert-Butyldimethylethylsilyl-6-O-benzylacycloguanosine, 10.** Compound **10** was prepared in analogy to the preparation of **7**, employing **9** (172 mg, 0.505 mmol), triphenylphosphine (266 mg, 1.0147 mmol), dry dioxane (8.7 mL), benzyl alcohol (105 μL, 1.0147 mmol), and diethylazodicarboxylate (464 μL, 1.0147 mmol). The crude product was purified by preparative TLC (1.5:4 hexane/ethyl acetate) to give 124.5 mg of white solid **10** (60% yield). <sup>1</sup>H NMR (500 MHz, *d*<sub>6</sub>-DMSO): δ 7.71 (s, 1H), 7.48 (d, *J* = 7.1 Hz, 2H), 7.33–7.24 (m, 3H), 5.56 (s, 2H), 5.49 (s, 2H), 4.92 (br, 2H), 3.71 (t, *J* = 4.7 Hz, 2H), 3.57 (t, *J* = 5.3 Hz, 2H), 0.86 (s, 9H), 0.027 (s, 6H). <sup>13</sup>C NMR (500 MHz, *d*<sub>6</sub>-DMSO): δ 161.2, 159.5, 154.3, 139.4, 136.4, 129.3, 128.4, 128.2, 128.0, 115.5, 72.9, 70.8, 68.1, 62.5, 25.9, 18.3, –5.3. ESI–HRMS: *m/e* 452.20677 (M + Na<sup>+</sup>) (calcd 452.208835).

**2-N-[2-(2'-O-tert-Butyldimethylethylsilyl-6-O-benzylacycloguanosyl)]-5'-O,3'-O,2'-O-tris(tert-butyldimethylethylsilyl)-6-O-benzylguanosine, 11.** In a dry flask, amine **10** (226.5 mg, 0.528 mmol), cesium carbonate (240.85 mg, 0.739 mmol, 1.4 equiv), palladium acetate (11.85 mg, 0.0528 mmol, 0.1 equiv), BINAP (49.32 mg, 0.0792 mmol, 0.15 equiv), bromide **8** (494.2 mg, 0.634 mmol, 1.2 equiv), and toluene (4.6 mL) were mixed under argon at room temperature for 30 min and then heated to 90 °C for 16 h. After the completion of the reaction, the reaction solution was diluted with ethyl acetate. The precipitate was removed by centrifugation, and the supernatant liquid was concentrated in vacuo. The residue was purified by flash chromatography (silica gel, 20–22% ethyl acetate/hexane) and afforded product **11** as a light-yellow oil (427.3 mg, 71.8% yield). <sup>1</sup>H NMR (500 MHz, CDCl<sub>3</sub>): δ 7.88 (s, 1H), 7.78 (s, 1H), 7.50 (m, 4H), 7.33–7.27 (m, 6H), 6.05 (d, *J* = 5.0 Hz, 1H), 5.77 (s, 2H), 5.68 (dd, *J* = 4.7, 12.5 Hz, 3H), 5.57 (dd, *J* = 13, 10.5 Hz, 2H), 4.52 (t, *J* = 4.5 Hz, 1H), 4.29 (t, *J* = 3.5 Hz, 1H), 4.08 (q, *J* = 2.5 Hz, 1H), 3.97 (dd, *J* = 11.5, 4.0 Hz, 1H), 3.77 (dd, *J* = 11.5, 2.5 Hz, 1H), 3.62 (t, *J* = 4.5 Hz, 2H), 3.52 (t, *J* = 5.5 Hz, 2H), 0.92 (d, *J* = 3.0 Hz, 18H), 0.82 (s, 9H), 0.78 (s, 9H), 0.11 (d, *J* = 3.5 Hz, 6H), 0.01 (s, 6H), –0.02 (s, 6H), –0.05 (s, 3H), –0.23 (s, 3H). <sup>13</sup>C NMR (500 MHz, *d*<sub>6</sub>-DMSO): δ 160.7, 160.6, 153.8,

153.7, 153.4, 153.3, 140.7, 139.5, 136.23, 136.20, 128.7, 128.4, 128.3, 128.1, 128.0, 117.5, 117.2, 87.8, 85.4, 76.3, 73.0, 72.1, 71.7, 70.6, 68.41, 68.36, 62.6, 62.4, 26.1, 25.9, 25.7, 18.6, 18.3, 18.1, 17.9, –4.4, –4.6, –4.7, –5.0, –5.1, –5.38, –5.40. ESI–HRMS: *m/e* 1150.58255 (M + Na<sup>+</sup>) (calcd 1150.580337).

**2-N-[2-(2'-O-tert-Butyldimethylethylsilylacycloguanosyl)]-5'-O,3'-O,2'-O-tris(tert-butyldimethylethylsilyl)guanosine, 12.** Compound **11** (427.3 mg, 0.378 mmol) was dissolved in 9.4 mL of THF, and 0.1 M tetrabutylammonium fluoride (TBAF) in THF solution (1.882 mL, 1.89 mmol) was added. The reaction solution was stirred for 1 h at 25 °C, then concentrated in vacuo, and the resulting residue was purified by flash chromatography (silica gel, 8% methanol/methene chloride) to give 30.7 mg product **8** (57.2%) as a white solid. <sup>1</sup>H NMR (500 MHz, *d*<sub>6</sub>-DMSO): δ 8.07 (s, 1H), 8.02 (s, 1H), 7.43 (d, *J* = 7.5 Hz, 4H), 7.28–7.22 (m, *J* = 6.1 Hz, 6H), 5.93 (d, *J* = 6.5 Hz, 1H), 5.68 (d, *J* = 3.0 Hz, 2H), 5.61 (d, *J* = 3.5 Hz, 2H), 5.58 (d, *J* = 3.0 Hz, 2H), 4.63 (t, *J* = 5.2 Hz, 2H), 4.52 (s, 1H), 4.27 (q, *J* = 2.1 Hz, 1H), 4.12 (d, *J* = 2.5 Hz, 1H), 3.70 (d, *J* = 2.8 Hz, 2H), 3.68 (d, *J* = 3.0 Hz, 1H), 3.65 (s, 1H), 3.60 (d, *J* = 3.0 Hz, 1H), 3.5 (s, 4H). <sup>13</sup>C NMR (500 MHz, *d*<sub>6</sub>-DMSO): δ 159.5, 153.0, 152.4, 140.9, 139.7, 135.6, 128.0, 127.9, 127.7, 127.6, 86.4, 77.5, 77.3, 77.0, 74.6, 72.6, 71.0, 70.4, 67.8, 60.4. ESI–HRMS: *m/e* 694.23341 (M + Na<sup>+</sup>) (calcd 694.234429).

**2-N-(2-Acycloinosyl)guanosine, rG-to-aG.** Ten percent palladium on activated carbon catalyst (104.5 mg) was added to a solution of **12** (321.4 mg, 0.479 mmol) in methanol (104.5 mL). The system was flushed with hydrogen gas three times before the reaction mixture was hydrogenated for 24 h at 60 psi with stirring. After completion of the reaction, the catalyst was removed by filtration through a pad of Celite. The filtrate was concentrated in vacuo; the crude product was purified by HPLC using analytical method A, and then desalted by HPLC employing analytical method B to yield 110.2 mg (87%) of **rG-to-aG** as a white solid. <sup>1</sup>H NMR (500 MHz, *d*<sub>6</sub>-DMSO): δ 8.15 (s, 1H), 8.09 (s, 1H), 5.78 (d, *J* = 5.5 Hz, 1H), 5.52 (s, 2H), 5.05 (s, 1H), 4.70 (s, 1H), 4.50 (s, 1H), 3.92 (q, *J* = 4.5 Hz, 1H), 3.72 (d, *J* = 10.0 Hz, 1H), 3.59 (t, *J* = 4.5 Hz, 2H), 3.55 (dd, *J* = 11.5, 3.5 Hz, 1H), 3.50 (s, 2H), 3.07 (q, *J* = 7.0 Hz, 1H). <sup>13</sup>C NMR (500 MHz, *d*<sub>6</sub>-DMSO): δ 149.0, 139.4, 137.8, 119.5, 119.0, 85.4, 73.7, 72.8, 71.0, 70.1, 61.4, 60.0. ESI–HRMS: *m/e* 514.14206 (M + Na<sup>+</sup>) (calcd 514.140529).

**rG-to-aG Formation by Guanosine Addition to Cyanoamine 4a.** 1-[(2-Hydroxyethoxy)methyl]-5-cyanoamine-4-imidazolecarboxamide (**4a**, 15 mg, 0.06 mmol) and guanosine (11 mg, 0.04 mmol) were added to 250 μL of DMSO, and the solution was stirred at 80 °C for 2 h. Then, 10 μL of the resulting light-yellow solution were diluted with 250 μL of DMSO for HPLC and LC–MS analyses using the analytical system 3 (vide supra) and an injection volume of 10 μL. The HPLC chromatogram of the reaction mixture showed the same peak that was observed for synthetic **rG-to-aG**, and the retention time was 16.0 min. To tune the mass spectrometer to optimal sensitivity, the solution of synthetic **rG-to-aG** was diluted to 0.02 mM, and at this concentration, the peaks of the synthetic cross-link and of the cross-link formed by the **rG** addition also agreed with regard to their intensity.

**Acknowledgment.** We are grateful for support by NIH Grant GM61027.

**Supporting Information Available:** <sup>1</sup>H and <sup>13</sup>C NMR spectra of **7–12** and **rG-to-aG**, and the results of the computational study. This material is available free of charge via the Internet at <http://pubs.acs.org>.

JA045108J